ACS OMEGA

Article

http://pubs.acs.org/journal/acsodf

Crystal Structure, Infrared Spectra, and Microwave Dielectric Properties of Temperature-Stable Zircon-Type (Y,Bi)VO_4 Solid-Solution Ceramics

Di Zhou,*[,†,‡] Jing Li,[†] Li-Xia Pang,[‡,§] Guo-Hua Chen,[∥] Ze-Ming Qi,[⊥] Da-Wei Wang,[‡] and Ian M. Reaney*[,‡]

[†]Electronic Materials Research Laboratory, Key Laboratory of the Ministry of Education & International Center for Dielectric Research, Xi'an Jiaotong University, Xi'an 710049, Shaanxi, China

[‡]Department of Materials Science and Engineering, University of Sheffield, Sheffield S1 3JD, U.K.

[§]Micro-optoelectronic Systems Laboratories, Xi'an Technological University, Xi'an 710032, Shaanxi, China

[∥]Guangxi Key Laboratory of Information Materials, Guilin University of Electronic Technology, Guilin 541004, Guangxi, China

[⊥]National Synchrotron Radiation Laboratory, University of Science and Technology of China, Hefei, Anhui 230029, China

ABSTRACT: A series of $(Bi_{1-x}Y_x)VO_4$ $(0.4 \leq x \leq 1.0)$ ceramics were synthesized using the traditional solid-state reaction method. In the composition range of $0.4 \leq x \leq 1.0$, a zircon-type solid solution was formed between 900 and 1550 °C. Combined with our previous work (scheelite monoclinic and zircon-type phases coexist in the range of $x < 0.40$), a pseudobinary phase diagram of $BiVO_4$–YVO_4 is presented. As x decreased from 1.0 to 0.40, the microwave permittivity (ε_r) of $(Bi_{1-x}Y_x)VO_4$ ceramics increased linearly from 11.03 to 30.9, coincident with an increase in the temperature coefficient of resonant frequency (TCF) from −61.3 to +103 ppm/°C. Excellent microwave dielectric properties were obtained for $(Bi_{0.3}Y_{0.7})VO_4$ sintered at 1025 °C and $(Bi_{0.2}Y_{0.8})VO_4$ sintered at 1075 °C with $\varepsilon_r \sim 19.35$, microwave quality factor (Qf) ~ 25 760 GHz, and TCF ~ +17.8 ppm/°C and $\varepsilon_r \sim 16.3$, Qf ~ 31 100 GHz, and TCF ~ −11.9 ppm/°C, respectively. Raman spectra, Shannon's additive rule, a classical oscillator model, and far-infrared spectra were employed to study the structure–property relations in detail. All evidence supported the premise that Bi-based vibrations dominate the dielectric permittivity in the microwave region.

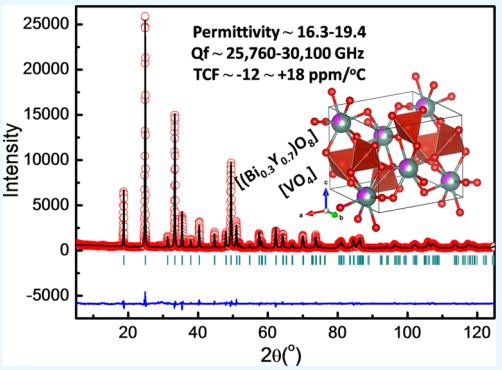

INTRODUCTION

Microwave dielectric ceramics have played an important role in modern wireless communication systems such as dielectric resonators, filters, capacitors, and duplexers. To meet the requirement of miniaturization and reliability of microwave devices, large dielectric permittivity (ε_r), large microwave quality factor (Qf), and near-zero temperature coefficient of resonant frequency (TCF) must be achieved.[1−4]

Many classic microwave dielectric ceramics based on ABO_3 perovskite structure have been explored, and the structure–property relation has been extensively studied.[5,6] Recently, many complex oxides with a classic ABO_4-type structure, such as scheelite ($CaMoO_4$, $BiVO_4$),[7,8] Fergusonite ($LaNbO_4$, $NdNbO_4$),[9] stibiotantalite ($BiNbO_4$, $BiTaO_4$),[10,11] wolframite ($ZnWO_4$, $MgWO_4$),[12] zircon ($CeVO_4$),[13] and rutile ((Zn,Nb)-TiO_4, (Cu,Nb)TiO_4)[14,15] structures, have been reported to have good microwave dielectric properties. Zircon-type ($I4_1/amd$) vanadates (AVO_4, A = Sc^{3+}, Ln^{3+}, Bi^{3+}) are a subset of ABO_4-type compounds and were widely investigated due to their potential optical, magnetic, elastic, and electric properties.[4,13] The zircon structure is composed of alternating $[VO_4]$ tetrahedra and edge-sharing $[AO_8]$ dodecahedra, forming chains parallel to the c axis. Two $[AO_8]$ dodecahedra are arranged along the a, b, and c axes, which results in a linear increase in cell volumes with A-site ionic radius.[4,16] As reported by Watanabe and Zuo,[13,17] $LaVO_4$ prefers to crystallize in a monoclinic monazite-type structure with a space group $P2_1/n$. The microwave dielectric properties of zircon-type $CeVO_4$ ceramics were first reported by Wang et al.[13] with a $\varepsilon_r \sim 12.3$, Qf ~ 41 460 GHz, and TCF ~ −34.4 at a sintering temperature of ~950 °C. It can be deduced that other rare-earth orthovanadates, such as YVO_4, $SmVO_4$, and $NdVO_4$, may also possess similar microwave dielectric properties. However, their large negative TCF values must be modified to near zero. There are two traditional methods to modify the TCF value of microwave dielectric ceramics to near zero, which are broadly separated into a composite and a solid-solution approach.[18] In our previous work, a temperature-stable microwave dielectric composite ceramic, which contains both scheelite $BiVO_4$ and zircon-type $(Bi_{0.6}Y_{0.4})VO_4$ phases with a $\varepsilon_r = 45$, Qf ~ 14 000

Received: September 29, 2016
Accepted: November 8, 2016
Published: November 18, 2016

DOI: 10.1021/acsomega.6b00274
ACS Omega 2016, 1, 963−970

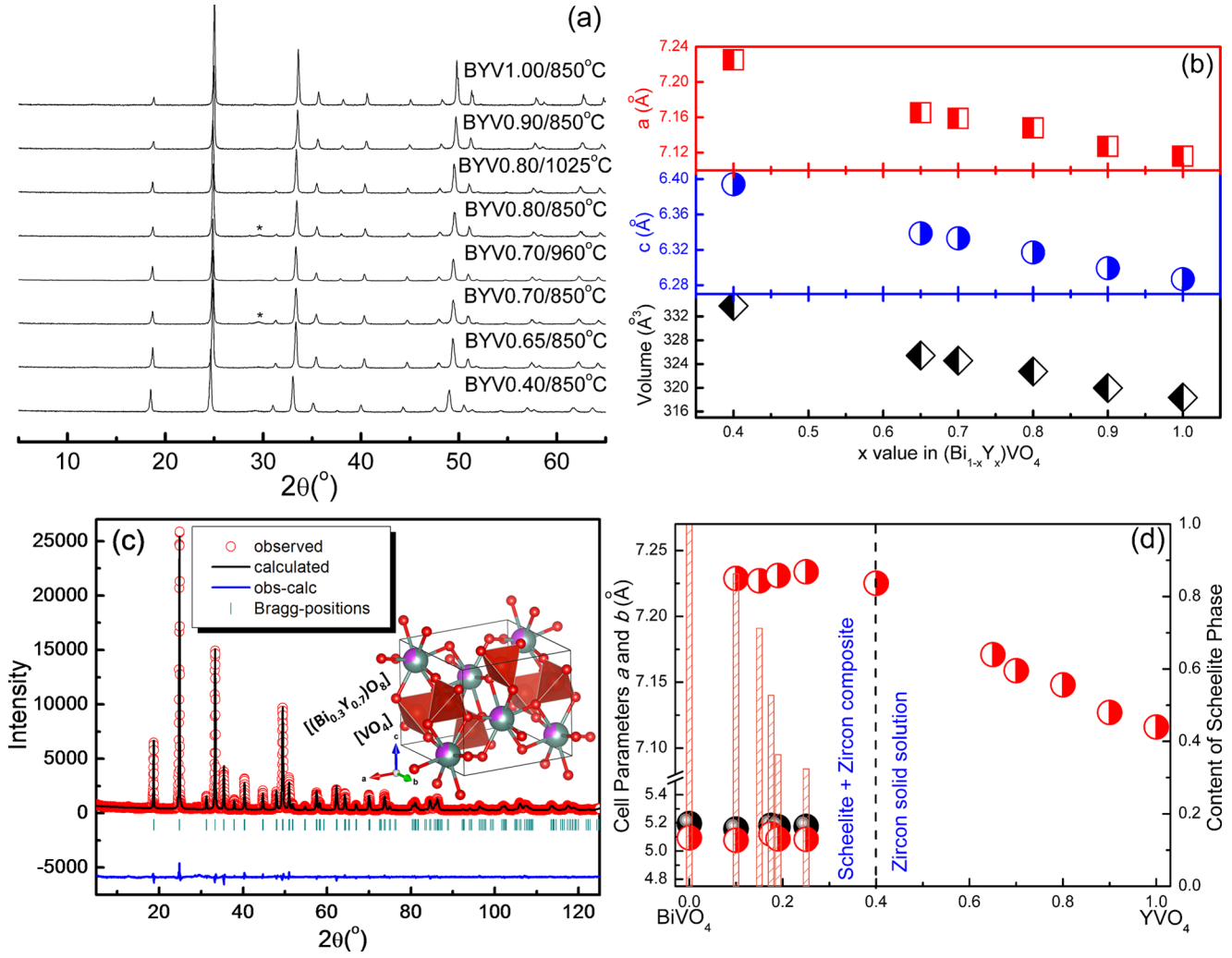

Figure 1. XRD patterns of $(Bi_{1-x}Y_x)VO_4$ ceramics calcined and sintered at different temperatures (a), cell parameters as a function of the x value (b), and experimental (circles) and calculated (line) X-ray powder diffraction profiles of the $(Bi_{0.3}Y_{0.7})VO_4$ composition sintered at 960 °C for 2 h at room temperature (c) (R_p = 12.7%, R_{wp} = 12.9%, R_{exp} = 7.27%). The short vertical lines below the patterns mark the positions of Bragg reflections. The bottom continuous line is the difference between the observed and the calculated intensity and the schematic phase diagram of the $BiVO_4$–YVO_4 system (d).

GHz, and TCF = +10 ppm/°C, was achieved.[4] The end member, $(Bi_{0.6}Y_{0.4})VO_4$, takes on the zircon structure with a positive TCF (+32 ppm/°C). This result inspired the design of a zircon-type solid-solution ceramic in the $(Bi,Y)VO_4$ system with a near-zero TCF. Undoped $BiVO_4$ ceramic prepared via the solid-state reaction method crystallizes in a monoclinic scheelite structure, not a zircon structure. As reported by Watanabe,[17] the solid solubility of the Bi^{3+} ion in zircon-structured $(Bi_xCe_{1-x})VO_4$ ceramics is ≥60%, as confirmed in our previous work,[19] which is attributed to the presence of the zircon-type $BiVO_4$ synthesized by a precipitation method.[20,21] Undoped zircon-type $BiVO_4$ is not stable and irreversibly transforms into a monoclinic scheelite structure at >300 °C,[21] and it is plausible that the substitution of Bi for Y in YVO_4 stabilizes the zircon-type lattice. In the present work, a comprehensive study on the phase assemblage and evolution in the $(Bi,Y)VO_4$ system was performed on the zircon-type solid-solution region and its associated sintering behavior, microstructure, and microwave dielectric properties were studied in detail.

RESULTS AND DISCUSSION

The X-ray diffraction (XRD) patterns of the $(Bi_{1-x}Y_x)VO_4$ ceramics calcined and sintered at their optimal temperatures are presented in Figure 1a. All peaks were indexed as a zircon-type phase for $x \geq 0.4$. As Bi concentration increased (decrease of x), all diffraction peaks shifted to the lower 2θ, commensurate with an increase in the cell volume, which is attributed to the larger ionic radius of Bi^{3+} (1.17 Å) compared with that of Y^{3+} (1.019 Å). The cell parameters of $(Bi_{1-x}Y_x)VO_4$ ($x \geq 0.4$) ceramics as a function of x value are presented in Figure 1b. a and c parameters increased from 7.116 to 7.225 Å and 6.287 to 7.394 Å, respectively, as x decreased from 1.0 to 0.4, commensurate with an increase in the cell volume from 318.35 to 333.79 Å^3. As shown in Figure 1c, the refined values of lattice parameters for the $(Bi_{0.3}Y_{0.7})VO_4$ sample are $a = b$ = 7.163(7) Å and c = 6.336(2) Å with a space group $I4_1/amd$ (141). All of the atomic fractional coordinates are listed in Table 1. The goodness of fit of refinement, which is defined as the ratio of R_{wp} to R_{exp}, is ~3.15. The V–O distance in the zircon-type $(Bi_{0.3}Y_{0.7})VO_4$ sample is 1.7005 Å, similar to that in YVO_4 (1.7058 Å). The long and short (Bi,Y)–O bond

DOI: 10.1021/acsomega.6b00274
ACS Omega 2016, 1, 963–970

Table 1. Refined Atomic Fractional Coordinates from XRD Data for the $(Bi_{0.3}Y_{0.7})VO_4$ Sample[a]

atom	site	occ.	x	y	z	biso.
Y	4a	0.08750	0.00000	0.75000	0.12500	0.27426
Bi	4a	0.03750	0.00000	0.75000	0.12500	0.27426
V	4b	0.12500	0.00000	0.25000	0.37500	0.14327
O	16h	0.50000	0.00000	0.06795	0.20273	0.12035

[a]The lattice parameters at room temperature are $a = b = 7.163(7)$ Å and $c = 6.336(2)$ Å with space group $I4_1/amd$ (141).

distances are 2.3301 and 2.4520 Å, respectively, which are larger than those in YVO_4 (2.2986 and 2.4434 Å, respectively),[22] consistent with the larger ionic radius of Bi^{3+} than that of Y^{3+}. Combined with our previous work,[4] the schematic phase diagram of the $(1 - x)BiVO_4$–$xYVO_4$ binary system is presented in Figure 1d. In the region $x \geq 0.4$, a zircon-type solid-solution phase field was formed. In the region $x < 0.4$, both monoclinic $BiVO_4$ and zircon $(Bi_{0.6}Y_{0.4})VO_4$ coexisted with stable cell parameters.

Undoped YVO_4 belongs to the D_{4h}^{19} crystal structure ($I4_1/amd$), and the theoretical group analysis gives an irreducible representation of the vibrational modes after Miller et al.[23] and Vali[24]

$$\Gamma_{36} = (2A_{1g} + 2B_{1u}) + (B_{1g} + A_{1u}) + (A_{2g} + B_{2u}) + (4B_{2g} + 4A_{2u}) + (5E_g + 5E_u) \quad (1)$$

The $2A_{1g}$, B_{1g}, B_{2g}, and $5E_g$ modes are the Raman-active optical modes, whereas the $3A_{2u}$ and $4E_u$ modes are infrared-active. In addition, there are two further inactive translational modes $A_{2u} + E_u$. As seen from Figure 2a, the main Raman modes created by stretching and bending of $[VO_4]$ tetrahedra at ~890, 378, 815, and 488 cm^{-1} are assigned to $A_{1g}(\nu_1)$, $A_{1g}(\nu_2)$, $B_{2g}(\nu_3)$, and $B_{2g}(\nu_4)$, respectively. The weak mode at 837 cm^{-1}, which is close to the $B_{2g}(\nu_3)$ mode, is assigned to E_g. The peaks at 260 cm^{-1} and overlapping at about 160 cm^{-1} are external modes caused by translation. As seen from Figure 2b, the main Raman modes shift to the lower wavenumber as x decreases, along with broadening and a decrease in peak intensity, due to the A-site disorder in the solid solution. According to Hardcastle and Wachs' study on the relation ($\nu = 21349\ e^{(-1.9176 \times R)}$),[25] in which ν is the Raman shift and R is the bond length of V–O) between the Raman shift and the V–O bond length, the decrease in the $A_{1g}(\nu_1)$ Raman mode (stretching mode of $[VO_4]$, Figure 2b) is caused by the increase in the V–O bond length.

Scanning electron microscopy (SEM) images of the $(Bi_{1-x}Y_x)VO_4$ ceramics are shown in Figure 3. For pure YVO_4 ($x = 1.0$), the densification temperature is above 1550 °C, and many pores are observed in ceramics sintered at 1550 °C for 2 h. As seen from Figure 3a–c, substitution of Bi for Y effectively lowered the sintering temperature and induced a homogeneous dense microstructure in $(Bi_{1-x}Y_x)VO_4$ ceramics with $x = 0.7$, 0.8, and 0.9. As x decreased from 1.0 to 0.7, the sintering temperatures of $(Bi_{1-x}Y_x)VO_4$ ceramics lowered from 1550 to 1025 °C along with a decrease in the grain size from ~5 to ~1 μm.

The microwave ε_r and Qf of the $(Bi_{1-x}Y_x)VO_4$ ceramics as a function of sintering temperature are shown in Figure 4. The ε_r of $(Bi_{1-x}Y_x)VO_4$ ceramics increased with sintering temperature due to the elimination of pores before reaching a stable value. The Qf increased with sintering temperature, reaching a maximum value before decreasing sharply for all samples except for $x = 1.0$. The Qf is composed of intrinsic and extrinsic contributions and affected by grain size, grain boundaries, and pores. For $(Bi_{1-x}Y_x)VO_4$ ceramics, high Qf values were attained only in a relatively narrow sintering temperature range. Optimal microwave properties of $(Bi_{1-x}Y_x)VO_4$ ceramics are listed in Table 2, in which ε_r decreases linearly from 30.9 at $x = 0.4$ to 11.1 at $x = 1.0$ in accordance with Shannon's additive rule. Shannon[26] suggested that polarizabilities of oxides may be estimated by summing the polarizabilities of constituent ions. The polarizabilities, α_x, of $(Bi_{1-x}Y_x)VO_4$ may be calculated as follows

$$\alpha_x = (1 - x) \times \alpha_{Bi^{3+}} + x\alpha_{Y^{3+}} + \alpha_{V^{5+}} + 4\alpha_{O^{2-}} \quad (2)$$

where $\alpha_{Bi^{3+}}$, $\alpha_{Y^{3+}}$, $\alpha_{V^{5+}}$, and $\alpha_{O^{2-}}$ are the polarizabilities of Bi^{3+}, Y^{3+}, V^{5+}, and O^{2-}, respectively. Because of smaller polarizabilities of Y^{3+} relative to those of Bi^{3+} ($\alpha_{Bi^{3+}} = 6.12^3$ Å $> \alpha_{Y^{3+}} = 3.81$ Å^3),[26] there should be a linear decrease in $(Bi_{1-x}Y_x)VO_4$ as x increases. Using the Clausius–Mossotti relation, which relates ε_x, α_x, and molar cell volume V_x, ε_r may be calculated

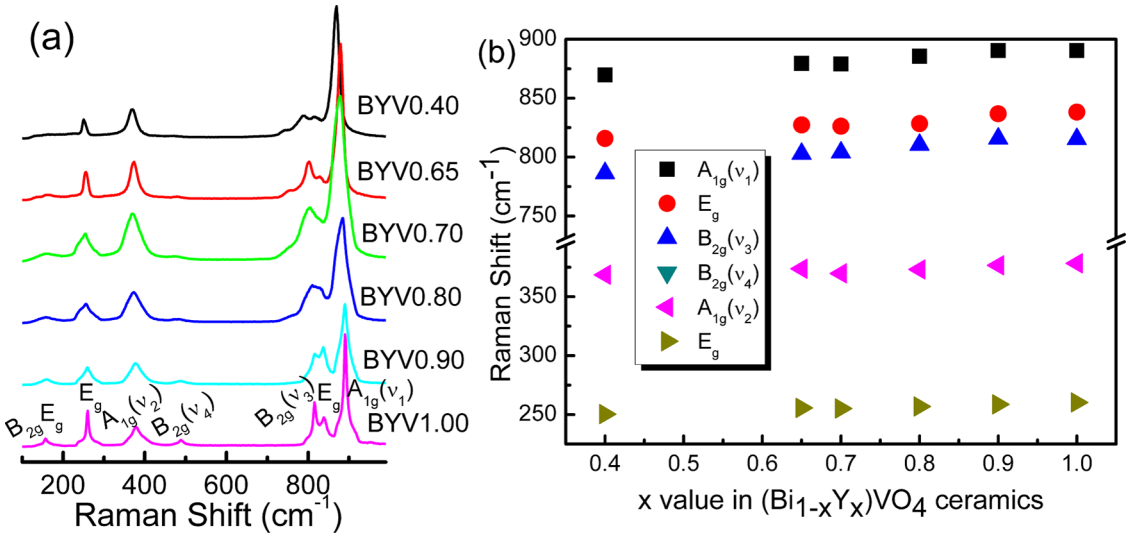

Figure 2. Raman spectra of $(Bi_{1-x}Y_x)VO_4$ ($x \geq 0.4$) ceramics (a) and as a function of the x value (b).

DOI: 10.1021/acsomega.6b00274
ACS Omega 2016, 1, 963–970

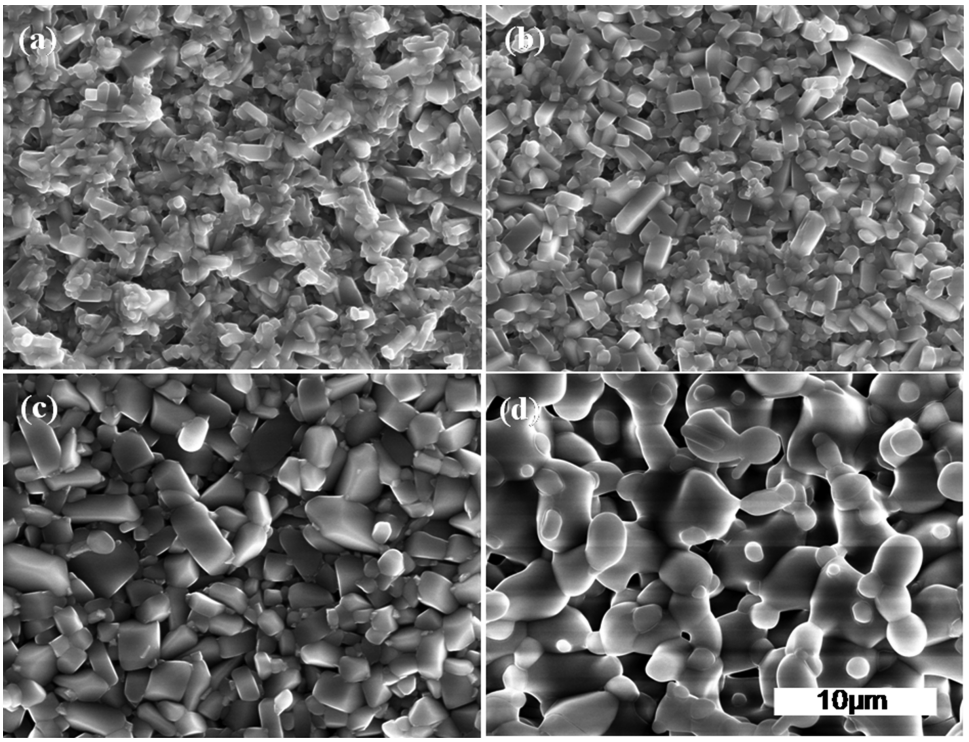

Figure 3. SEM images of $(Bi_{1-x}Y_x)VO_4$ ceramics sintered at different temperatures: x = 0.70 at 1025 °C (a), 0.80 at 1075 °C (b), 0.90 at 1225 °C (c), and 1.00 at 1550 °C (d).

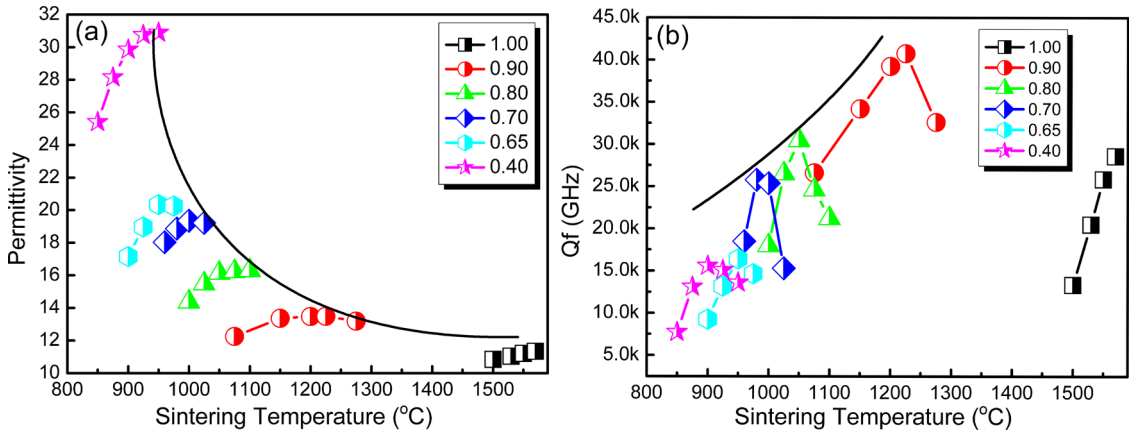

Figure 4. Microwave dielectric permittivity (a) and Qf values (b) of $(Bi_{1-x}Y_x)VO_4$ ceramics as a function of sintering temperature.

Table 2. Densification Temperature, Microwave Dielectric Properties, and Molecular Polarizability of the $(Bi_{1-x}Y_x)VO_4$ Ceramics

x	S.T. (°C)	ε_r	Qf (GH)	TCF (ppm/°C)	V (Å^3)	$\alpha_{cal.}$ (Å^3)	$\alpha_{meas.}$ (Å^3)
0.4	975	30.9	15 570	+103	333.79	16.16	18.11
0.65	995	20.5	16 380	+32	325.43	15.58	16.83
0.7	1025	19.35	25 760	+17.8	324.55	15.46	16.65
0.8	1075	16.3	30 100	−11.9	322.76	15.23	16.11
0.9	1225	13.49	40 720	−31.2	319.96	15.00	15.40
1.0	1550	11.03	28 600	−61.3	318.35	14.77	14.63

$$\varepsilon_x = \frac{3V_x + 8\pi\alpha_x}{3V_x - 4\pi\alpha_x} \Leftrightarrow \alpha_x = \frac{3V_x}{4\pi}\frac{\varepsilon_x - 1}{\varepsilon_x + 2} \quad (3)$$

The values of molecular α_x calculated from eqs 2 and 3 along with the macroscopic microwave dielectric properties are listed in Table 2. As x decreases, the relative deviation between $\alpha_{cal.}$ and $\alpha_{meas.}$ increases. Employing eq 3, it can be obtained that $\alpha_{Bi^{3+}} - \alpha_{Y^{3+}} = (\alpha_{x2} - \alpha_{x1})/(x_1 - x_2) \approx 5.8$ Å^3. This result is greater than that reported by Shannon (2.31 Å^3), which suggests that within its coordination in the zircon-type structure, Bi^{3+} contributes much more than Y^{3+} to the dielectric polarizability, compared with that in higher-symmetry systems.

DOI: 10.1021/acsomega.6b00274
ACS Omega 2016, 1, 963−970

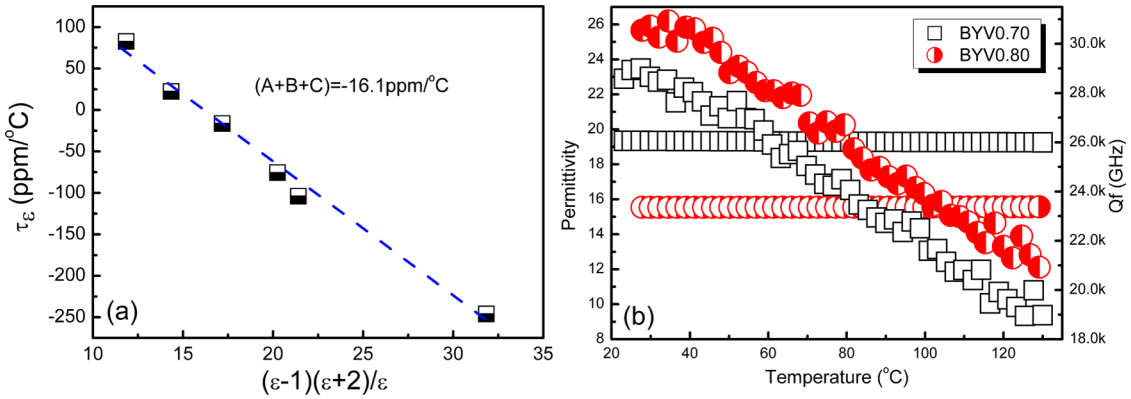

Figure 5. τ_ε (temperature dependence of permittivity) as a function of $(\varepsilon - 1)(\varepsilon + 2)/\varepsilon$ (a) and permittivity and Qf as a function of temperature (b) for the $(Bi_{0.3}Y_{0.7})VO_4$ and $(Bi_{0.2}Y_{0.8})VO_4$ ceramics.

The highest Qf (~40 700 GHz) was obtained for $(Bi_{0.1}Y_{0.9})VO_4$, but as x decreased to 0.65 and 0.40, the Qf decreased linearly to 16 000 GHz. The intrinsic dielectric loss determines the upper limit of Qf and is quantitatively described by the classical one-phonon damped oscillator model as follows[27]

$$\varepsilon^*(\omega) - \varepsilon(\infty) = \frac{(ze)^2/mV\varepsilon_0}{\omega_T^2 - \omega^2 - j\gamma\omega} \tag{4}$$

where $\varepsilon^*(\omega)$ is the complex permittivity, $\varepsilon(\infty)$ is the electronic part of the static permittivity, ε_T is the transverse frequency of the polar phonon mode, γ is the damping parameter, z is the equivalent electric charge number, e is the electric charge of an electron, m is the equivalent atom weight, and V is the unit volume. In the microwave region, considering $\omega^2 \ll \omega_T^2$, the relationship between the Qf and ε_r is obtained as follows

$$Q \times f \approx \frac{(ze)^2/mV\varepsilon_0}{2\pi\gamma \times (\varepsilon'(\omega) - \varepsilon(\infty))} \tag{5}$$

The above relation was successfully used to explain the reciprocal relationship between the ε_r and Qf in scheelite solid solutions.[28] The same qualitative relationship holds for zircon-type solid solutions in $(Bi_{1-x}Y_x)VO_4$ ceramics. The decrease in Qf for undoped YVO_4 is attributed to the absence of a sintering temperature, at which the density of the end member compound may be optimized. The TCF of undoped YVO_4 is ~−61.3 ppm/°C. As x decreased to 0.40, the TCF linearly increased to +103 ppm/°C. In contrast, +17.8 and −11.9 ppm/°C were obtained in the $(Bi_{0.3}Y_{0.7})VO_4$ and $(Bi_{0.2}Y_{0.8})VO_4$ ceramics, respectively, suggesting that zero TCF may be achieved for $0.7 < x < 0.8$. The TCF is usually defined as follows

$$\mathrm{TCF} = -\alpha_l - \frac{1}{2}\tau_\varepsilon \tag{6}$$

where α_l is the thermal expansion coefficient and τ_ε is the temperature coefficient of dielectric constant. Usually α_l of microwave dielectric is <+20 ppm/°C and independent of x. Hence, the TCF value mainly depends on τ_ε. Using the Clausius−Mosotti relation, Bosman and Havinga[29] derived an expression for τ_ε at constant pressure as follows

$$\tau_\varepsilon = \frac{1}{\varepsilon}\left(\frac{\partial\varepsilon}{\partial T}\right)_P = \frac{(\varepsilon - 1)(\varepsilon + 2)}{\varepsilon}(A + B + C)$$
$$= \left(\varepsilon - \frac{2}{\varepsilon} + 1\right)(A + B + C) \tag{7}$$

$$A = \frac{1}{3V}\left(\frac{\partial V}{\partial T}\right)_P,\quad B = \frac{1}{3\alpha_m}\left(\frac{\partial\alpha_m}{\partial V}\right)_T\left(\frac{\partial V}{\partial T}\right)_P,$$
$$C = \frac{1}{3\alpha_m}\left(\frac{\partial\alpha_m}{\partial T}\right)_V$$

The sum of the A and B terms is approximately 6 ppm/°C. Term C usually lies between −1 and ~−10 ppm/°C and represents the direct dependence of the polarizability on temperature. Figure 5a shows a plot of the temperature dependence of permittivity (α_l was assumed to be +20 ppm/°C) as a function of $(\varepsilon - 1)(\varepsilon + 2)/\varepsilon$ for all of the $(Bi_{1-x}Y_x)VO_4$ ceramics to extrapolate the $(A + B + C)$ value ~ −16.1 ppm/°C, which is within the acceptable range. Using this relation, any TCF value can be achieved by precisely adjusting the composition. Furthermore, it is similar to the empirical logarithmic rule ($\ln\varepsilon = y_1 \ln\varepsilon_1 + y_2 \ln\varepsilon_2$/TCF $= y_1 \ln\tau_{f1} + y_2 \ln\tau_{f2}$)[30] suitable for composites. The temperature dependence of the ε_r and Qf of the $(Bi_{0.3}Y_{0.7})VO_4$ and $(Bi_{0.2}Y_{0.8})VO_4$ ceramics in the temperature range 25−130 °C is shown in Figure 5b. ε_r is stable at ~19 and 16 for the $(Bi_{0.3}Y_{0.7})VO_4$ and $(Bi_{0.2}Y_{0.8})VO_4$ ceramics, respectively. Qf decreased linearly with temperature from 28 000 to ~20 000 GHz, confirming that the dielectric loss increased with temperature. Taking into account the above arguments, temperature-stable microwave dielectric ceramics may be obtained for $0.7 < x < 0.8$ with $16 \le \varepsilon_r \le 19$ and Qf > 20 000 GHz between 25 and 130 °C. The sintering temperature of this system (below 1050 °C) is much lower than that of $SrLnAlO_4$ (Ln = Nd and Sm) microwave dielectric ceramics[31] (1475−1500 °C) with similar properties (permittivity 17.8−18.8, Qf values 25 700−54 880 GHz, and TCF values −9 ~ +2 ppm/°C), and this can save a lot of energy during processing.

Far-infrared reflectivity is a useful tool to investigate intrinsic dielectric properties of microwave ceramics. As discussed above, there are seven infrared-active modes including three A_{2u} and four E_u modes. In Vali et al.'s work,[24] a perpendicular electric field of the incident light to the c axis of YVO_4 single crystal was employed to obtain the infrared reflectivity and only four E_u modes, at 195, 263, 309, and 780 cm^{-1}, were observed. As

DOI: 10.1021/acsomega.6b00274
ACS Omega 2016, 1, 963−970

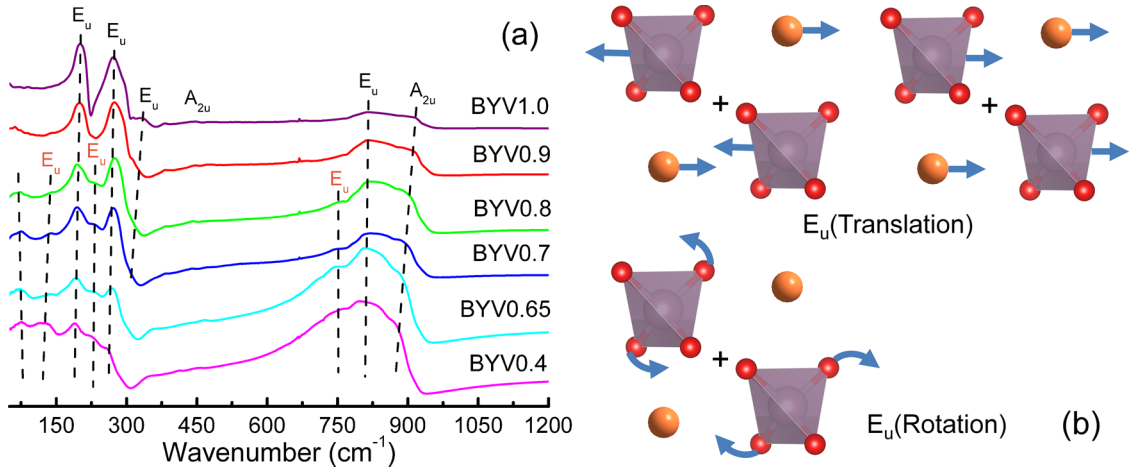

Figure 6. Far-infrared reflectivity of $(Bi_{1-x}Y_x)VO_4$ ceramics (a) and schematic of external E_u modes caused by translation and rotation (b).

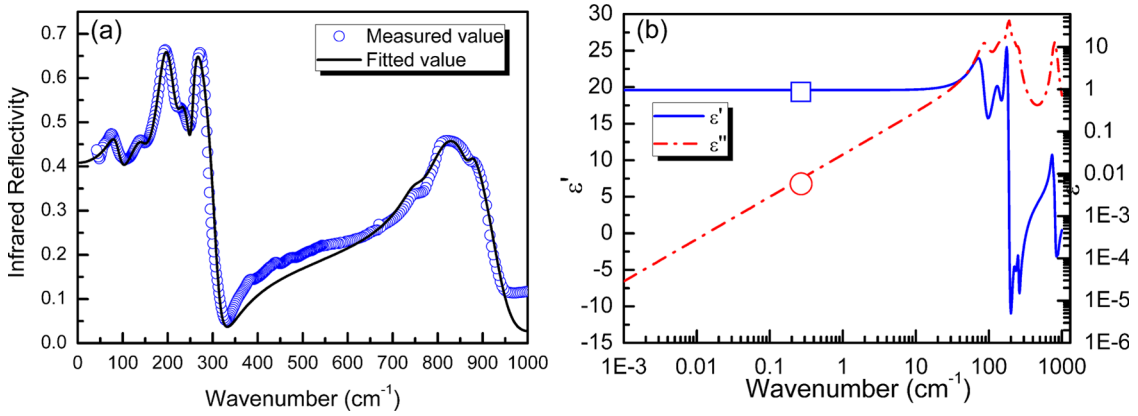

Figure 7. Measured and calculated infrared reflectivity spectra (a) (solid line for fitting values and circle for measured values) and fitted complex dielectric spectra (b) of the $(Bi_{0.3}Y_{0.7})VO_4$ ceramic (the circles represent the experimental values in the microwave region).

shown in Figure 6, besides the four E_u modes, two other modes at 439 and 916 cm^{-1}, assigned to A_{2u} modes, were also observed to contribute to the infrared reflectivity spectra of the YVO_4 ceramic sample. The high wavenumber peak at 916 cm^{-1} belongs to the stretching mode of $[VO_4]$, which is similar to that at 977 cm^{-1} caused by the Si−O stretching in $ZrSiO_4$ material.[31,32] As x decreased to 0.8, four new modes are observed, at 69, 136, 233, and 749 cm^{-1}. These new modes are also assigned to E_u modes caused by the partial occupation by Bi on the A site of the zircon structure. The external E_u modes below 450 cm^{-1} are conventionally caused by translation and rotation between A-site ions and $[VO_4]$ tetrahedra, as shown in Figure 6b. Because of the different relative masses of Bi and Y atoms, the translation and rotation strengths are different and lead to different Raman shifts; consequently, the strength of the E_u modes increased with Bi concentration.

Using eq 4, the relation between complex reflectivity $R(\omega)$ and permittivity can be obtained as follows

$$R(\omega) = \left| \frac{1 - \sqrt{\varepsilon^*(\omega)}}{1 + \sqrt{\varepsilon^*(\omega)}} \right|^2 \quad (8)$$

The fitting of infrared reflectivity was employed to study the intrinsic dielectric contribution from each vibrational mode. Infrared reflectivity spectra of $(Bi_{0.3}Y_{0.7})VO_4$ were fitted using eight modes as shown in Figure 7a, and the related parameters are listed in Table 3. Among the eight modes, Nos. 1, 2, 4, and 6 belong to Bi-based vibrations, and their total contribution to the microwave permittivity was ∼8, whereas all others were attributed to the Y-based and $[VO_4]$ tetrahedral vibrations (value about ∼7.2). The optical permittivity is ∼4.41. This result indicates that Bi-based vibrations mainly contribute to permittivity in the microwave region, in accordance with the analysis using Shannon's additive rule. The measured and fitted real and imaginary parts of permittivity are plotted in Figure 7b. The measured part corresponded well with the fitted values,

Table 3. Phonon Parameters Obtained from the Fitting of the Infrared Reflectivity Spectra of the $(Bi_{0.3}Y_{0.7})VO_4$ Ceramic[a]

mode	ω_{oj}	ω_{pj}	γ_j	$\Delta\varepsilon_j$
1	**86.97**	**170.99**	**32.31**	**3.77**
2	**142.85**	**245.14**	**45.68**	**2.74**
3	187.97	444.15	26.78	5.38
4	**229.35**	**266.24**	**39.57**	**1.25**
5	256.07	168.85	15.32	0.44
6	**750.00**	**365.67**	**54.21**	**0.24**
7	803.83	967.63	93.02	1.35
8	871.76	154.23	32.06	0.03
	ε_∞ = 4.41		ε_0 = 19.61	

[a]Bold type represents the modes coming from Bi-based vibrations.

DOI: 10.1021/acsomega.6b00274
ACS Omega 2016, 1, 963−970

confirming that in the microwave region the dielectric polarization is mainly caused by phonon absorption in the infrared region.

CONCLUSIONS

A zircon-type solid solution is formed in $(Bi_{1-x}Y_x)VO_4$ ($0.4 \le x \le 1.0$) ceramics. Substitution of Bi effectively lowered sintering temperatures from above 1550 °C for undoped YVO_4 to ~900 °C for $(Bi_{0.6}Y_{0.4})VO_4$. As x decreased from 1.0 to 0.4, cell parameters increased linearly, along with the increase of ε_r from 11.03 to 30.9 accompanied by a shift of TCF value from −61.3 to +103 ppm/°C. Excellent microwave dielectric properties with a $\varepsilon_r \sim 19.35$, Qf ~ 25 760 GHz, and TCF ~ +17.8 ppm/°C were obtained in $(Bi_{0.3}Y_{0.7})VO_4$ ceramic sintered at 1025 °C. For $(Bi_{0.2}Y_{0.8})VO_4$ ceramic sintered at 1075 °C, $\varepsilon_r \sim 16.3$, Qf ~ 31 100 GHz, and TCF ~ −11.9 ppm/°C were obtained. It is demonstrated that temperature-stable microwave dielectric ceramics can be obtained for compositions with $0.7 < x < 0.8$. Therefore, we conclude, with reference to our previous work,[4] that there are two methods to design temperature-stable microwave dielectric ceramics in the $(Bi_{1-x}Y_x)VO_4$ system for gigahertz frequency applications: (1) the fabrication of composites of scheelite and zircon phases and (2) the formation of zircon-structured solid solution with $0.7 < x < 0.8$.

EXPERIMENTAL SECTION

The $(Bi_{1-x}Y_x)VO_4$ (x = 0.4, 0.65, 0.7, 0.8, 0.9, and 1.0) (abbreviated BYVx) samples were prepared via the solid-state reaction method as described in our previous work.[2,3] Samples were sintered at temperatures from 850 to 1550 °C for 2 h.

XRD was performed with Cu Kα radiation (Rigaku D/MAX-2400 X-ray diffractometry, Tokyo, Japan) using a powder sample. The diffraction pattern was collected over 5−65° (2θ) at a step size of 0.02°. The Rietveld profile refinement method was employed to analyze the data using the FULLPROF program. As-fired surfaces were observed by SEM (FEI; Quanta 250 F). Raman spectra were performed with a Raman spectrometer (inVia; Renishaw, England), excited by an Ar^+ laser (514.5 nm). Infrared reflectivity spectra were measured using a Bruker IFS 66v FT-IR spectrometer on the infrared beamline station (U4) at the National Synchrotron Radiation Lab. (NSRL), China. Microwave dielectric properties were measured using the $TE_{01\delta}$ method with a network analyzer (HP 8720 Network Analyzer; Hewlett-Packard) and a temperature chamber (Delta 9023; Delta Design, Poway, CA). The temperature coefficient of resonant frequency TCF (τ_f) was calculated with the following formula

$$\mathrm{TCF}(\tau_f) = \frac{f_T - f_{T_0}}{f_{T_0} \times (T - T_0)} \times 10^6 \quad (9)$$

where f_T and f_{T_0} are the $TE_{01\delta}$ resonant frequencies at temperatures T and T_0, respectively.

AUTHOR INFORMATION

Corresponding Authors

*E-mail: zhoudi1220@gmail.com. Tel/Fax: +86-29-82668679 (D.Z.).

*E-mail: i.m.reaney@sheffield.ac.uk (I.M.R.).

ORCID

Di Zhou: 0000-0001-7411-4658

Notes

The authors declare no competing financial interest.

ACKNOWLEDGMENTS

This work was supported by the National Natural Science Foundation of China (U1632146), the Young Star Project of Science and Technology of Shaanxi Province (2016YFXX0029), the Fundamental Research Funds for the Central University, Guangxi Key Laboratory of Information Materials (Guilin University of Electronic Technology), P.R. China (Project No. 161004-K), and the 111 Project of China (B14040). The authors would like to thank the administrators of the IR beamline workstation of the National Synchrotron Radiation Laboratory (NSRL) for their help. The SEM work was done at the International Center for Dielectric Research (ICDR), Xi'an Jiaotong University, Xi'an, China, and the authors thank Yan-Zhu Dai for her help in using SEM.

REFERENCES

(1) Reaney, I. M.; Iddles, D. Microwave Dielectric Ceramics for Resonators and Filters in Mobile Phone Networks. *J. Am. Ceram. Soc.* **2006**, *89*, 2063−2072.

(2) Sebastian, M. T.; Jantunen, H. Low loss dielectric materials for LTCC applications: a review. *Int. Mater. Rev.* **2008**, *53*, 57−90.

(3) Zhou, D.; Guo, D.; Li, W. B.; Pang, L. X.; Yao, X.; Wang, D. W.; Reaney, I. M. Novel temperature stable high-ε_r microwave dielectrics in the Bi_2O_3−TiO_2−V_2O_5 system. *J. Mater. Chem. C* **2016**, *4*, 5357−5362.

(4) Zhou, D.; Li, W. B.; Xi, H. H.; Pang, L. X.; Pang, G. S. Phase composition, crystal structure, infrared reflectivity and microwave dielectric properties of temperature stable composite ceramics (scheelite and zircon-type) in $BiVO_4$-YVO_4 system. *J. Mater. Chem. C* **2015**, *3*, 2582−2588.

(5) Scott, R. I.; Thomas, M.; Hampson, C. Development of low cost, high performance $Ba(Zn_{1/3}Nb_{2/3})O_3$ based materials for microwave resonator applications. *J. Eur. Ceram. Soc.* **2003**, *23*, 2467−2471.

(6) Jancar, B.; Valant, M.; Suvorov, D. Solid-State Reactions Occurring during the Synthesis of $CaTiO_3$-$NdAlO_3$ Perovskite Solid Solutions. *Chem. Mater.* **2004**, *16*, 1075−1082.

(7) Choi, G. K.; Kim, J. R.; Yoon, S. H.; Hong, K. S. Microwave dielectric properties of Scheelite (A = Ca, Sr, Ba) and wolframite (A = Mg, Zn, Mn) AMoO4 compounds. *J. Eur. Ceram. Soc.* **2007**, *27*, 3063−3067.

(8) Zhou, D.; Pang, L. X.; Guo, J.; Qi, Z. M.; Shao, T.; Yao, X.; Randall, C. A. Phase evolution, phase transition, and microwave Dielectric properties of scheelite structured $xBi(Fe_{1/3}Mo_{2/3})O_4 - (1-x)BiVO_4$ ($0.0 \le x \le 1.0$) low temperature firing ceramics. *J. Mater. Chem.* **2012**, *22*, 21412−21419.

(9) Kim, D. W.; Kwon, D. K.; Yoon, S. H.; Hong, K. S. Microwave Dielectric Properties of Rare-Earth Ortho-Niobates with Ferroelasticity. *J. Am. Ceram. Soc.* **2006**, *89*, 3861−3864.

(10) Zhou, D.; Wang, H.; Yao, X. Microwave dielectric properties and co-firing of $BiNbO_4$ ceramics with CuO substitution. *Mater. Chem. Phys.* **2007**, *104*, 397−402.

(11) Huang, C. L.; Weng, M. H. Low-fire $BiTaO_4$ dielectric ceramics for microwave applications. *Mater. Lett.* **2000**, *43*, 32−35.

(12) Yoon, S. H.; Kim, D. W.; Cho, S. Y.; Hong, K. S. Investigation of the relations between structure and microwave dielectric properties of divalent metal tungstate. *J. Eur. Ceram. Soc.* **2006**, *26*, 2051−2054.

(13) Wang, Y.; Zuo, R.; Zhang, C.; Zhang, J.; Zhang, T. Low-Temperature-Fired $ReVO_4$ (Re = La, Ce) Microwave Dielectric Ceramics. *J. Am. Ceram. Soc.* **2015**, *98*, 1−4.

(14) Pang, L. X.; Wang, H.; Zhou, D.; Yao, X. Sintering behavior, structures and microwave dielectric properties of a rutile solid solution system: $(A_xNb_{2x})Ti_{1-3x}O_2$ (A = Cu, Ni). *J. Electroceram.* **2009**, *23*, 13−18.

DOI: 10.1021/acsomega.6b00274
ACS Omega 2016, 1, 963−970

(15) Kim, E. S.; Kang, D. H. Relationships between crystal structure and microwave dielectric properties of $(Zn_{1/3}B_{2/3}^{5+})_xTi_{1-x}O_2$ (B^{5+} = Nb, Ta) ceramics. *Ceram. Int.* **2008**, *34*, 883−888.
(16) Jindal, R.; Sinha, M. M.; Gupta, H. C. Lattice vibrations of AVO_4 crystals (A = Lu, Yb, Dy, Tb, Ce). *Spectrochim. Acta, Part A* **2013**, *113*, 286−290.
(17) Watanabe, A. Highly Conductive Oxides, $CeVO_4$, $Ce_{1-x}M_xVO_{4-0.5x}$(M = Ca, Sr, Pb) and $Ce_{1-y}Bi_yVO_4$, with Zircon-Type Structure Prepared by Solid-State Reaction in Air. *J. Solid State Chem.* **2000**, *153*, 174−179.
(18) Zhou, D.; Pang, L. X.; Wang, H.; Guo, J.; Yao, X.; Randall, C. A. Phase transition, Raman spectra, infrared spectra, band gap and microwave dielectric properties of low temperature firing $(Na_{0.5x}Bi_{1-0.5x})(Mo_xV_{1-x})O_4$ solid solution ceramics with scheelite structure. *J. Mater. Chem.* **2011**, *21*, 18412−18420.
(19) Zhou, D.; Pang, L. X.; Guo, J.; Qi, Z. M.; Shao, T.; Wang, Q. P.; Xie, H. D.; Yao, X.; Randall, C. A. Influence of Ce Substitution for Bi in $BiVO_4$ and the Impact on the Phase Evolution and Microwave Dielectric Properties. *Inorg. Chem.* **2014**, *53*, 1048−1055.
(20) Bhattacharya, A. K.; Mallick, K. K.; Hartridge, A. Phase transition in $BiVO_4$. *Mater. Lett.* **1997**, *30*, 7−13.
(21) Kudo, A.; Omori, K.; Kato, H. A Novel Aqueous Process for Preparation of Crystal Form-Controlled and Highly Crystalline $BiVO_4$ Powder from Layered Vanadates at Room Temperature and Its Photocatalytic and Photophysical Properties. *J. Am. Chem. Soc.* **1999**, *121*, 11459−11467.
(22) Baglio, J. A.; Sovers, O. J. Crystal structures of the rare-earth orthovanadates. *J. Solid State Chem.* **1971**, *3*, 458−465.
(23) Miller, S. A.; Caspers, H. H.; Rast, H. E. Lattice Vibrations of Yttrium Vanadate. *Phys. Rev.* **1968**, *168*, 964−969.
(24) Vali, R. Ab initio vibrational and dielectric properties of YVO_4. *Solid State Commun.* **2009**, *149*, 1637−1640.
(25) Hardcastle, F. D.; Wachs, I. E. Determination of Vanadium-Oxygen Bond Distances and Bond Orders by Raman Spectroscopy. *J. Phys. Chem.* **1991**, *95*, 5031−5041.
(26) Shannon, R. D. Dielectric polarizabilities of ions in oxides and fluorides. *J. Appl. Phys.* **1993**, *73*, 348−366.
(27) Petzelt, J.; Kamba, S. Submillimetre and infrared response of microwave materials: Extrapolation to microwave properties. *Mater. Chem. Phys.* **2003**, *79*, 175−180.
(28) Zhou, D.; Wang, H.; Wang, Q. P.; Wu, X. G.; Guo, J.; Zhang, G. Q.; Shui, L.; Yao, X.; Randall, C. A.; Pang, L. X.; Liu, H. C. Microwave dielectric properties and Raman spectroscopy of scheelite solid solution $[(Li_{0.5}Bi_{0.5})_{1-x}Ca_x]MoO_4$ ceramics with ultra-low sintering temperatures. *Funct. Mater. Lett.* **2010**, *3*, 253−257.
(29) Bosman, A. J.; Havinga, E. E. Temperature Dependence of Dielectric Constants of Cubic Ionic Compounds. *Phys. Rev.* **1963**, *129*, 1593−1600.
(30) Pang, L. X.; Wang, H.; Zhou, D.; Yao, X. A new temperature stable microwave dielectric with low-firing temperature in Bi_2MoO_6-TiO_2 system. *J. Alloys Compd.* **2010**, *493*, 626−629.
(31) Chen, X. M.; Xiao, Y.; Liu, X. Q.; Hu, X. $SrLnAlO_4$ (Ln = Nd and Sm) microwave dielectric ceramics. *J. Electroceram.* **2003**, *10*, 111−115.
(32) Pecharroman, C.; Ocana, M.; Tartaj, P.; Serna, C. J. Infrared optical properties of zircon. *Mater. Res. Bull.* **1994**, *29*, 417−426.

DOI: 10.1021/acsomega.6b00274
ACS Omega 2016, 1, 963−970